Testing ecological interactions between Gnomoniopsis castaneae and Dryocosmus kuriphilus

(Article begins on next page)

07 January 2023

UNIVERSITÀ DEGLI STUDI DI TORINO

1

2

3

4

13

Testing ecological interactions between *Gnomoniopsis castaneae* and *Dryocosmus kuriphilus*

Guglielmo Lione[a], Luana Giordano[a,b], Chiara Ferracini[a], Alberto Alma[a] and Paolo Gonthier[a]

[a] Department of Agricultural, Forest and Food Sciences, University of Torino, Largo Paolo Braccini 2, 10095 Grugliasco, Italy

[b] Centre of Competence for the Innovation in the Agro-Environmental Field (AGROINNOVA), University of Torino, Largo Paolo Braccini 2, 10095 Grugliasco, Italy

Corresponding author: Paolo Gonthier (paolo.gonthier@unito.it)

Role of Authors

GL and LG conducted samplings and fungal isolations. GL performed statistical analyses and LG molecular diagnostics assays. GL and PG designed the experiments and wrote the manuscript. CF helped with the manipulation of insects and with the interpretation of results. AA supervised the work on insects and revised the manuscript.

34   **Abstract**

35

36   An emerging nut rot of chestnut caused by the fungus *Gnomoniopsis castaneae*

37   was reported soon after the invasion of the exotic gall wasp *Dryocosmus kuriphilus* in

38   Italy. The goal of this work was to assess the association between the spread of the

39   fungal pathogen and the infestation of the pest by testing if:

40   I) viable inoculum of *G. castaneae* can be carried by adults of *D. kuriphilus*;

41   II) the fungal colonization is related to the number of adults inhabiting the galls;

42   III) the fungal colonization of chestnut buds and the oviposition are associated.

43   Fungal isolations and PCR-based molecular assays were performed on 323

44   chestnut galls and on their emerging *D. kuriphilus* adults, whose number was compared

45   between galls colonized and not colonized by *G. castaneae*. To test the association

46   between fungal colonization and oviposition, Monte Carlo simulations assuming

47   different scenarios of ecological interactions were carried out and validated through

48   isolation trials performed on 597 and 688 chestnut buds collected before and after

49   oviposition, respectively.

50   Although DNA of *G. castaneae* was detected in a sample of 40% of the adults

51   developed in colonized galls, the fungus could never be isolated from insects,

52   suggesting that the pest is an unlikely vector of viable inoculum.

53   On average, the emerging adults were significantly more abundant from galls

54   colonized by *G. castaneae* than from not colonized ones (3.76 *vs.* 2.54, P<0.05),

55   indicating a possible fungus/pest synergy.

56   The simulations implying no interaction between *G. castaneae* and *D. kuriphilus*

57   after fungal colonization were confirmed as the most likely. In fact, *G. castaneae* was

58   present in 33.8% of the buds before oviposition, while no association was detected

59   between fungal colonization and oviposition (odds ratio 0.98, 0.71-1.33 95% CI). This

60   finding suggests that the fungus/pest synergy is asymmetrically favorable to the pest

61   and occurs after oviposition.

62

63   **Keywords**: *Dryocosmus kuriphilus,* fungi, *Gnomoniopsis castaneae, Gnomoniopsis*

64   *smithogilvyi,* insects, Monte Carlo

65

66   **1. Introduction**

67

68   Interspecific interactions stand among the major forces driving the ecosystem

69   dynamics and resulting in effects which are perceptible at both structural and functional

70   levels (Jones et al., 1994; Tilman, 1999). Interactions between plant pathogens and

71   insects have been well-documented in agricultural and forest ecosystems as pivotal

72   factors enhancing the occurrence, the transmission and the spread of plant diseases.

73   Pathogenic fungi (Paine et al., 1997; Carlile et al., 2001; Harrington, 2013), bacteria

74   (Harrison et al., 1980; Redak et al., 2004), phytoplasmas (Griffiths, 2013) and viruses

75   (Spence, 2001) can be carried and released by insects through mechanical, metabolic,

76   physiological, or trophic processes, depending on the case.

77   For some infectious diseases of trees, the ecological association relating fungal

78   pathogens to insects has been identified as one of the main underlying features of the

79   epidemiological processes. For instance, many fungal plant pathogens release volatile

80   organic compounds that are highly attractive to some mycophagous insects. During the

81   feeding process, the spores of the pathogen come into contact with the insects and can

82   adhere on the surface of their exoskeleton, be collected in specialized anatomical

83   structures or transported within the insect body. Subsequently, the contaminated insects

84   may allow the fungal dispersal and transmit the pathogen from tree to tree, often

85   through preexisting fresh wounds (Happ et al., 1971; Webber, 2004; Kirisits, 2013;

86   Harrington, 2013).

87   The role played by the insects in the ecological association with fungal

88   pathogens may extend beyond the transportation and the release of the spores. In fact,

89   the vectors are often pests attacking the same host of the pathogen, leading to complex

90   network of pest-pathogen-host interactions. For instance, pathogenic fungi requiring

91   fresh wounds on the host tissues to start the infection process can be directly inoculated

92   by their vectors during the excavation of galleries generated for feeding or breeding.

93   While the fungal mycelium colonizes the host, the pests can take advantage of its

94   presence either through the direct consumption of the fungus (i.e. mycophagia), or by

95   feeding on an altered substrate with improved nutritional qualities (Paine et al., 1997).

96   The synergy between the pathogen and the vector explains their mutual escalation,

97   whose natural limitation relies in the increased death rate and in the alteration of the

98   age structure occurring in the host trees population (Webber, 2004; Danti et al., 2013;

99   Eckhardt, 2013; Kirisits, 2013).

100   Despite rarely documented, pests can also activate latent pathogens, whose

101   switch from the endophytic to the pathogenic phase may be associated with the

102   physiological reaction of the host to the pest attack (Sieber and Hugentobler, 1987).

103   The fungal-insect ecological interactions may explain the association between

104   the spread of emerging pathogens and the biological invasion of exotic pests (Kirisits,

105   2013). Since 2005, a severe epidemic of nut rot has spread throughout the populations

106   of the European chestnut (*Castanea sativa* Miller) in Italy, and its causal agent was

107   described for the first time in 2012 as *Gnomoniopsis castaneae* G. Tamietti (syn: *G.*

108   *smithogilvyi* L.A. Shuttlew., E.C.Y. Liew & D.I. Guest), an ascomycete included in the

109   family of Gnomoniaceae (Visentin et al., 2012; Tamietti, 2016). *G. castaneae* is

110   currently regarded as a major pathogen of chestnut in Italy, France and Switzerland

111   (Visentin et al., 2012; Maresi et al., 2013; Dennert et al., 2015; Lione et al., 2015; Lione

112   and Gonthier, 2016). Despite the pathogen lives as a parasite inside the kernel of the

113   nut, it can also be isolated from the buds, the leaves, the bark of juvenile sprouts and

114   from other green tissues of the tree where it does not induce any symptom. While

115   fruiting bodies of the sexual form of *G. castaneae* can be observed on the burr

116   surrounding the nut, the asexual stage of the fungus produces its multiplicative

117   structures on the galls of *Dryocosmus kuriphilus* Yasumatsu (Visentin et al., 2012;

118   Maresi et al., 2013). *D. kuriphilus*, commonly known as the Asian chestnut gall wasp, is

119   a pest belonging to Hymenoptera Cynipidae that was accidentally introduced to Europe

120   in the early 2000s (Quacchia et al., 2008). In the summer, *D. kuriphilus* lays eggs into

121   the buds of chestnut, where its larvae overwinter. During the following vegetative

122   season, the larvae develop within cells located in the inner tissues of the galls inducing

123   the formation of greenish-red galls, suppressing shoot elongation and causing twig

124   dieback (Ôtake, 1980). New adults emerge from the galls in the summer. A massive

125   presence of galls results in a dramatic reduction of the photosynthetic area, inhibits the

126   growth of the tree, decreases the chestnut vigor and determines substantial yield losses

127   (Kato and Hijii, 1997; EFSA, 2010; Sartor et al., 2015). Severe reduction of fruiting

128   estimated between 65% and 85% was observed in northern Italy, but recently the

129   presence of the pest has significantly decreased thanks to the biological control

130   programs performed with the Hymenoptera Torymidae *Torymus sinensis* Kamijo

131   (Ferracini et al., 2015).

132   Based on the first confirmed reports of the presence of *G. castaneae* and *D.*

133   *kuriphilus* in the European chestnut populations, the invasion of the pathogen occurred

134   a few years after the invasion of the pest and started in the same areas located in the

135   Cuneo Province, in north-western Italy (Brussino et al., 2002; Visentin et al., 2012),

136   suggesting that possible interactions between the pathogen and the pest may occur.

137   Although galls necrosis along with mortality of *D. kuriphilus* were observed in

138   association with *G. castaneae* (Magro et al., 2010), the ecological interaction between

139   the fungal pathogen and the exotic pest still remains widely unexplored.

140   The main goal of this work was to test some among the possible ecological

141   interactions between *G. castaneae* and *D. kuriphilus* by combining theoretical and

142   empirical approaches. In detail, three specific hypotheses of ecological interactions

143   were tested:

144   I)   whether viable inoculum of *G. castaneae* can be carried by adults of *D. kuriphilus*;

145   II) whether the colonization of the gall tissues by *G. castaneae* is related to the number

146   of inhabiting adults of *D. kuriphilus*;

147   III) whether the fungal colonization of plant buds and the oviposition by the insect are

148   associated.

149

2. Methods

151

2.1. Experimental design

153

154   In each of the three sites located in north-western Italy (Table 1), five chestnuts

155   were randomly selected. Branches with a maximum diameter of 1 cm harbored most *D.*

156   *kuriphilus* galls and chestnut buds (see below), and thus were deemed to be

157   representative for sampling purposes. From the crown of each tree, 10 branches were

158   excised during two distinct samplings, the first one performed on 20th June 2013, before

159   the oviposition timeframe of *D. kuriphilus*, while the second one was carried out on 25th

160   September 2013, after the oviposition timeframe. The approximate starting date and the

161   length of the oviposition timeframe were estimated according to EPPO (2005) and Alma

162   et al. (2014).

163

2.2. Biological analyses

165

166   During the first sampling, 323 galls of *D. kuriphilus* were collected (up to two galls

167   per branch, if present) and incubated separately into aerated plastic cages stored at

168 room temperature (~25±2 °C) and normal daylight exposure. The cages were visually

169 inspected twice a day, for 3 weeks, and the 35% of the emerging adults of *D. kuriphilus*

170 was plated into 6 cm diameter Petri dishes to isolate *G. castaneae* according to the

171 protocol described in Giordano et al. (2013). The remaining adults were individually

172 transferred using sterile tweezers into sterile 1.5 mL microcentrifuge tubes and stored at

173 -20 °C. After 5 days without new emerging adults, the galls were removed from their

174 incubator. In order to isolate *G. castaneae*, 5 fragments of approximately 5 × 5 × 1 mm

175 were randomly excised from both the inner and the outer tissues of each gall and plated

176 into 9 cm diameter Petri dishes filled with malt extract agar (MEA) (Visentin et al., 2012).

177   The isolation trials described above for the galls were performed on 597 and 688

178 buds (up to 5 buds per branch) after the first and the second sampling, respectively. A

179 subset of 60 buds collected from the former sampling and all the buds obtained from the

180 latter were sectioned under a dissecting microscope (20 × magnification) to assess the

181 presence of *D. kuriphilus* eggs.

182   For both samplings, the identification of the pathogen was performed based on

183 the macro and micro-morphological features of growing colonies, as described in

184 Visentin et al. (2012) and Lione et al. (2015).

185

186 **2.3. Molecular analyses**

187

188   A subset of 40 insects, half emerged from galls colonized by *G. castaneae* and

189 half from galls not colonized (see Results), was drawn from the adults of *D. kuriphilus*

190 previously stored at -20 °C. On this subset, PCR-based molecular analyses were

191 performed to validate the results of the isolation trials (i.e. molecular validation). Fungal

192 DNA extraction was carried out by using the E.Z.N.A.™ Stool DNA Isolation Kit (Omega

193 Bio-Tek, Norcross, GA, USA) following the manufacturer's instructions. *G. castaneae*

194 was identified through a taxon-specific molecular diagnostic assay. The two primers

195 Gc1f (5'-AGCGGGCATGCCTGTTCGAG-3') and Gc1r (5'-

196 ACGGCAAGAGCAACCGCCAG-3') were used as described in Lione et al. (2015) to

197 specifically detect *G. castaneae*. All PCRs were carried out by setting the thermocycler

198 parameters as follows: an initial 95°C denaturation step of 5 min, followed by 35 cycles

199 of 95 °C denaturation for 30 s, 62 °C annealing for 45 s and 72 °C extension for 1 min,

200 and a final 72 °C extension step of 10 min. The specific amplicon of *G. castaneae* (168

201 bp) was visualized in gel containing 1% (w/v) of high resolution MetaPhor (Cambrex)

202 and 1% (w/v) of standard agarose, after electrophoretic migration. In order to assess the

203 efficiency of fungal DNA extraction, an additional PCR amplification of the Internal

204 Transcribed Spacer (ITS) was performed with the universal primers ITS1 and ITS4

205 (White et al., 1990; Gardes et al., 1991).

206   Moreover, the above cited taxon-specific molecular assay was carried out on a

207 random subset of 50 putative colonies of *G. castaneae* to confirm the morphological

208 identifications.

209

210 **2.4. Statistical analysis and Monte Carlo simulations**

211

212   According to the results of the isolation trial, the galls were classified as

213 colonized (GC^+) or not colonized (GC^-) by *G. castaneae*. Negative binomial generalized

214 linear regression models (nbGLM), parametrized with the intercept, were run to

215 compare the average number of adults of *D. kuriphilus* emerged from GC$^+$ (codified as

216 1) and GC$^-$ (codified as 0) (Venables and Ripley, 2002; Kéry, 2010). One nbGLM per

217 site and an overall model for the three sites were fitted.

218   In both GC$^+$ and GC$^-$, the proportion (%) of *D. kuriphilus* adults positive to *G.*

219 *castaneae* (A$^+$) was calculated separately for the isolation trial and for the molecular

220 validation along with the exact 95% confidence intervals (95% CI) obtained as reported

221 by Blaker (2000). The proportion of A$^+$ was compared between GC$^+$ and GC$^-$ with the

222 Fisher's exact test (Crawley, 2013).

223   A Monte Carlo (MC) experiment (Carsey and Harden, 2014) was set to test *in*

224 *silico* the association between the colonization of *G. castaneae* and the oviposition by

225 *D. kuriphilus*. An artificial environment was designed to simulate the oviposition and the

226 fungal colonization processes at buds level. In a cubic Cartesian space with edges

227 bounded between 0 and 40 cm, three branches of 35 cm, each one with three twigs of 5

228 cm were designed. A single branch included 20 buds, while 5 buds were located along

229 each twig, achieving a total of 105 buds. The probability density functions (PDFs) of the

230 distances separating two consecutive buds on the branches and on the twigs were

231 estimated through the fit of the distribution types included in the Pearson system

232 (Pearson, 1895; Lachene, 2013). The fit was performed on the pooled distances

233 measured on four model branches and on their twigs collected in the field during the

234 first sampling. The optimal Pearson type PDF was selected according to the minimum

235 Akaike Information Criterion (AIC) (Akaike, 1973; Crawley, 2013). Two scenarios of

236 asymmetric association (Somers, 1962) between fungal colonization and oviposition,

237 and between oviposition and fungal colonization were simulated: scenario A) the fungal

238 colonization may influence the insect oviposition; scenario B) the insect oviposition may

239 influence the fungal colonization. Each scenario was simulated under two competing

240 hypotheses. In the scenario A, the hypothesis A_1 assumed that the buds colonized

241 (BC^+) and not colonized (BC^-) by *G. castaneae* were equally attractive to *D. kuriphilus*,

242 while under the alternative hypothesis A_2 the BC^+ were more likely to attract ovipositing

243 insects than BC^-. Similarly, in the scenario B, the buds oviposited (BO^+) were as

244 attractive to the fungus as the not oviposited ones (BO^-), under the hypothesis B_1, while

245 BO^+ were more attractive to *G. castaneae* than BO^-, under the competing hypothesis

246 B_2. For the scenario A, the attraction exerted by the buds was modelled as a series

247 spherical buffers (Mitchell, 1999). Each spherical buffer was centered in the associated

248 bud coordinates, while the radius was weighted differently according to the hypothesis

249 being simulated. The radius was set constant at 0.5 cm for all the buds under A_1, while

250 under A_2 it was set to 0.5 cm for BC^- and to 1 cm for BC^+. For the scenario B, the

251 attraction was modeled as a numeric weight assigned to the buds. Under B_1 the weight

252 was set to 0.5 in order to assign to all buds an even probability of extraction regardless

253 of the oviposition status. The probability of extraction was automatically rescaled by the

254 sampling algorithm based on random number generators (Mitchell, 2005; Carsey and

255 Harden, 2014). Under B_2 the weight was tuned to 0.2 for BO^- and to 0.8 for BO^+ in order

256 to simulate a different attraction, depending on the oviposition status, without

257 introducing an asymmetry hyperparameter (i.e. different attractiveness weights were

258 evenly spaced around the equal attractiveness weight) (Mitchell, 2005; Kéry, 2010;

259 Carsey and Harden, 2014). The oviposition process of a single adult of *D. kuriphilus*

260   was simulated by modelling the insect trajectory as a Lévy flight. The Lévy flight was

261   generated as a three dimensional random walk whose steps were derived from a

262   power-law tailed PDF, with parameter a=1 and μ=2, and whose zenith and azimuth

263   were drawn, at each step, from a uniform distribution bounded between 0 and 2π

264   radians (Reynolds and Frye, 2007; Edwards, 2008; Kéry, 2010). The status BO^+ was

265   assigned to the bud whose buffer included for the first time the ending point of a single

266   step of the Lévy flight. The fungal colonization was modelled as a stochastic process,

267   based on a random number generator, drawing buds and assigning to them the BC^+

268   status according to an extraction probability proportional to a weight (Carsey and

269   Harden, 2014). The weight was attributed to the buds depending on the hypothesis

270   being tested (see below). Within each hypothesis the ratio between BC^+ and the total

271   buds (i.e. g) was set to g = 20%, 40%, 60%, 80%. Similarly, the number of adults was

272   set as a proportion of the maximum number of buds that could be oviposited in percent,

273   selecting for this percent (d) the same values attributed to g (i.e. d = 20%, 40%, 60%,

274   80%). Each combination between g and d and the additional combination g=50% and

275   d=60% were set as a couple of fixed parameters to run a block of 5000 Monte Carlo

276   (MC) simulations. Within each hypothesis, 17 blocks of MC simulation were run, for a

277   total of $3.4 \cdot 10^5$ simulations (2 scenarios · 2 hypotheses · 17 blocks · 5000 simulations).

278   In the scenario A, each MC simulation consisted in the following steps: 1) drawing the g

279   BC^+ after the fungal colonization process was run with a weight set constant for all the

280   105 buds; 2) running d independent oviposition processes of a single adult of *D.*

281   *kuriphilus* to gather BO^+, with the radii of the spherical buffers set as described above

282   for each hypothesis; 3) cross-tabulating the BC^+, BC^-, BO^+ and BO^- and calculating the

283   odds ratio θ as the measure of association between fungal colonization and oviposition

284   (Agresti, 2001). Every MC simulation in the scenario B was performed through the

285   following steps: 1) retrieving the BO^+ from A_1, step 2; 2) running the fungal colonization

286   process with the weights assigned to BO^+ and BO^-, depending on the buds attraction

287   tuned according to hypotheses described above, and drawing the g BC^+; 3-4) replicating

288   previous steps 3 and 4. The 5000 θ values obtained within the blocks were used to

289   estimate the PDFs of the odds ratios, whose average $\bar{\theta}$ was calculated with its 95% CI

290   lower and upper bounds (i.e. $\bar{\theta}_l$ and $\bar{\theta}_u$) (Buckland, 1983; Jones et al., 2009). MC

291   algorithms were run in R 3.2.1. (scripts are available as Supplementary Material

292   Appendix A).

293   The MC simulations were biologically validated with the results gathered during

294   the isolation trials performed on the buds. For both samplings, the ratio g_o between BC^+

295   and the total buds was calculated with its 95% CI (Blaker, 2000) separately for each site

296   and conjointly for all sites. The g_o values were compared between the two samplings

297   with the Fisher's exact test. For the second sampling, the ratio d_o between BO^+ and the

298   total buds was calculated as described for g_o. The fungal colonization and the

299   oviposition status of the buds were cross-tabulated and the odds ratio θ_o with its 95% CI

300   (i.e. θ_{ol} and θ_{ou}) were calculated with the Fisher's method. Subsequently, θ_o, θ_{ol} and θ_{ou}

301   were compared to the average odds ratios and their associated 95% CI obtained from

302   the MC simulations (Agresti, 2001; Carsey and Harden, 2014). The comparison was

303   performed by assessing the probability (L) of gathering *in silico* an outcome statistically

304   equivalent to the values obtained through the field samplings and the laboratory

305   analyses, conditional to the occurrence of each hypothesis (i.e. the likelihood of θ_o, θ_{ol}

306   and θ_{ou}). L was calculated within the hypotheses as the relative frequency of MC

307   simulation blocks whose θ, θ_l and θ_u were statistically equivalent to θ_o, θ_{ol} and θ_{ou} (i.e.

308    $L = \frac{\sum I(\theta_l < 1 < \theta_u)}{17}$ if $\theta_{ol} < 1 < \theta_{ou}$, $L = \frac{\sum I(\theta_l > 1)}{17}$ if $\theta_{ol} > 1$, otherwise $L = \frac{\sum I(0 < \theta_u < 1)}{17}$, where I is

309   the indicator function according to Iverson's notation) (Gerber et al., 2003; Kéry, 2010;

310   Carsey and Harden, 2014).

311   A threshold of 0.05 was set as cut-off for the rejection of the null hypotheses of

312   all statistical tests.

313

314   **3. Results**

315

316   The taxon-specific molecular assay confirmed the morphological identifications of

317   all the putative colonies of *G. castaneae* tested. The isolation trial performed on the

318   galls resulted in 120 GC[+] and 203 GC[-], with a ratio between GC[+] and total number of

319   galls ranging from 16.0% to 67.7%, depending on the site. A total of 966 adults of *D.*

320   *kuriphilus* emerged from the galls, 451 from GC[+] and 515 from GC[-]. On average, the

321   insects from GC[+] were significantly more abundant than the ones emerged from GC[-]

322   (2.62-3.90 *vs.* 0.62-2.89, P<0.05), as shown by the P-values displayed by the β

323   coefficients in all the nbGLM (Table 2).

324   On the subset of adults scored for the presence of *G. castaneae*, 180 emerged

325   from GC[+] and 159 from GC[-]. The proportion of A[+] assessed through the isolation trial

326   was 0% both for *D. kuriphilus* adults emerged from GC[+] (0-2.0% 95% CI) and for adults

327   deriving from GC[-] (0-2.2% 95% CI), resulting in a not significant Fisher's exact test

328   (P>0.05). On the contrary, the proportion of A[+] determined through the molecular assay

15

329   raised to 40.0% (20.9-63.1% 95% CI) for the adults from GC[+], remaining stable at 0%

330   (0-16.0% 95% CI) for the others. The former proportion resulted significantly larger than

331   the latter (P<0.05).

332   The optimal fits for the PDFs of the distances separating two consecutive buds

333   corresponded to Pearson type III curves with shape, location and scale parameters of

334   1.89, 2.07 and 12.6 for the branches (AIC=435.3), and 2.20, -0.16, 5.72 for the twigs

335   (AIC=182.1). Depending on the g-d combination, the blocks of MC simulations

336   displayed mean values $\bar{\theta}$ of odds ratios ranging from 0.127 to 1.394 under the

337   hypothesis A_1, and $\bar{\theta}$ values comprised between 1.07 and 1.34 under the hypothesis

338   B_1. Under A_1, the 95% CI associated with $\bar{\theta}$ showed bounds comprised within the

339   ranges 0-0.46 for $\bar{\theta}_l$ and 1.47-5.46 for $\bar{\theta}_u$, while under B_1 the bounds ranged from 0.18

340   to 0.46 for $\bar{\theta}_l$ and from 2.14 to 5.68 for $\bar{\theta}_u$. No significant association between the

341   colonization of *G. castaneae* and the oviposition by *D. kuriphilus* emerged under both A_1

342   and B_1, since the value 1 was comprised between $\bar{\theta}_l$ and $\bar{\theta}_u$ in all blocks. Under the

343   alternative hypotheses, the corresponding g-d blocks of MC simulations displayed

344   ranges from 2.24 to 8.50 for $\bar{\theta}_l$, from 4.78 to 35.47 for $\bar{\theta}$ and from 6.25 to 102.5 for $\bar{\theta}_u$

345   in A_2, and from 1.60 to 5.44 for $\bar{\theta}_l$, from 5.74 to 21.86 for $\bar{\theta}$ and from 7.90 to 60.80 for

346    $\bar{\theta}_u$ in B_2. A positive and significant association between fungal colonization and the

347   oviposition arose, since the condition $1 \leq \bar{\theta}_l$ occurred in all blocks simulated under A_2

348   and B_2 (Table 3).

349   Depending on the site, the ratio g_o was comprised between 1.1% and 52.2%, and

350   between 30.7% and 48.5% in the first and in the second sampling, respectively,

351   displaying a significant increase only in the site of Aymavilles (P<0.05). The overall ratio

352   of g_o attained 33.8% in the first sampling and 40.7% in the second one, showing a

353   significant raise between samplings (P<0.05) (Fig. 1). The subset of buds inspected for

354   *D. kuriphilus* eggs showed the absence of oviposition in all buds collected during the

355   first sampling. Instead, in the second sampling, the values displayed by the ratio d_o were

356   87.1% (82.0-91.2% 95% CI) in Aymavilles, 96.1% (92.8-98.2% 95% CI) in Nomaglio

357   and 0% (0-1.6% 95% CI) in Robilante, with an overall value of 61.0% (57.3-64.7% 95%

358   CI). The odds ratio θ_o obtained for the sites of Aymavilles (1.45, 0.59-3.58 95% CI),

359   Nomaglio (0.75, 0.14-3.56 95% CI) as well as the overall value (0.98, 0.71-1.33 95% CI)

360   were not significantly different from 1 (P>0.05). Instead, the corresponding value for

361   Robilante could not be estimated since no oviposited buds were detected in the second

362   sampling. The values of L were calculated according to the fact that the overall and

363   within site 95% CI satisfied the condition $\theta_{ol} < 1 < \theta_{ou}$. In all cases, L attained the value

364   100% under A_1 and B_1, and 0% under the competing hypotheses.

365

4. Discussion

367

368   The spread of plant pathogens and the invasion of exotic pests may be closely

369   associated, especially if they share the same hosts. Often, pathogen-pest ecological

370   interactions have been proved to drive the spread of both the pathogen and the pest.

371   Pathogens and pests can operate in synergy through a series of processes leading to

372   mutual advantages, to the detriment of the host plant. In the case of fungal plant

373   pathogens, pests can operate as vectors of viable inoculum, as agents responsible for

374   the inoculation process and as constructors of micro-environments favorable to the

375 fungal colonization and reproduction. In return, the pathogen can alter the physical and

376 the chemical qualities of the host tissues, providing the pests with an improved

377 substrate for feeding and breeding. In some cases, the fungus may also represent a

378 trophic resource for mycophagous insects (Paine et al., 1997; Webber, 2004; Danti et

379 al., 2013; Eckhardt, 2013; Harrington, 2013; Kirisits, 2013).

380   The spatial and temporal overlaps between the outbreak of the nut rot of the

381 European chestnut caused by *G. castaneae* and the biological invasion of *D. kuriphilus*

382 occurring in Italy suggest a possible association between the emerging fungal pathogen

383 and the exotic pest. The isolation trials indicate that *D. kuriphilus* is unlikely to carry

384 viable inoculum of *G. castaneae*. In fact, if the pest was a vector, a certain amount of

385 adults emerged from the colonized galls (GC[+]) should have resulted positive to *G.*

386 *castaneae*. Instead, the fungus was never isolated from the adults of *D. kuriphilus*,

387 regardless of the presence or absence of viable inoculum colonizing the gall tissues. On

388 the contrary, DNA of *G. castaneae* could be detected in a subset of the insects emerged

389 from the colonized galls. These findings may indicate that, when *G. castaneae*

390 colonizes the gall tissues, the emerging adults of *D. kuriphilus* are potentially able to

391 carry a certain amount of inoculum. However, this inoculum is no longer viable and,

392 consequently, it cannot contribute to the infection process and to the spread of the

393 pathogen. Despite the separation between the putative inoculum present in the inner

394 tissues of the insect body from the inoculum adhering on the exoskeleton was not

395 performed, the isolation technique was suitable to reveal the presence of both, since the

396 insects were mostly smashed during the plating process because of their structural

397 fragility. However, since *D. kuriphilus* consumes part of the inner tissues of the galls, the

398   inoculum of *G. castaneae* in the form of mycelium might have been ingested and

399   subsequently inactivated during the digestive processes, rather than transported on the

400   surface of the exoskeleton. It should be noted that no specialized anatomical structures

401   allowing fungal inoculum transportation are present on the exoskeleton of *D. kuriphilus*.

402   The significantly larger number of adults of *D. kuriphilus* hosted in the galls

403   colonized by *G. castaneae* could be the result of an interaction occurring between the

404   fungus and the pest during oviposition. *G. castaneae* colonizing the buds could exert an

405   attractive effect towards the pest, yet also the oviposited buds could represent a more

406   favorable environment for the fungal colonization. Testing these hypotheses *in silico*

407   through Monte Carlo methods was advantageous, since such methods allowed to

408   model and simulate iteratively the ecological phenomena (i.e. oviposition/colonization

409   and attractiveness of oviposited/colonized buds) under different scenarios (i.e. influence

410   of fungal colonization on oviposition, or influence of oviposition on fungal colonization)

411   and with various combinations of biologically relevant parameters (i.e. number of adults

412   and colonized buds). The oviposition by *D. kuriphilus* and the fungal colonization were

413   modeled as stochastic processes based on Lévy flight and on random sampling from

414   probability distributions, respectively. Despite the absence of studies specifically

415   focused on *G. castaneae* and *D. kuriphilus*, these approaches have been proved to be

416   effective and consistent with in-field observations when simulating the flight trajectory of

417   insects and the dynamics of fungal colonization in several natural and semi-natural

418   ecosystems (Reynolds and Frye, 2007; Edwards, 2008; Honkaniemi et al., 2014;

419   Jarnevich and Young, 2015). Also the assignment of differential weights and the

420   delimitation of buffers to model the buds attractiveness towards the fungus and the

421 insect were consistent with the methods proposed in the literature to investigate

422 ecological interactions (Mitchell, 1999; Mitchell, 2005; Gonthier et al., 2012). Regardless

423 of the scenario and of the number of adults and colonized buds, the outcomes of the

424 simulations (i.e. average odds ratios and associated 95% CI) showed that the

425 association between fungal colonization and oviposition by *D. kuriphilus* depends on

426 which hypothesis about the attraction exerted by the oviposited/colonized buds on the

427 fungus/pest is assumed. When modelling all the buds as equally attractive, no

428 ecological association between the two phenomena could be detected, meaning that no

429 interaction between *G. castaneae* and *D. kuriphilus* occurred. Conversely, when the

430 oviposited/colonized buds were modeled as more attractive to the fungus/pest,

431 significant and positive average odds ratios were displayed, indicating the existence of

432 an underlying interaction between *G. castaneae* and *D. kuriphilus*. The biological

433 validation is a pivotal step to carry out when testing hypotheses through MC simulations

434 (Thébaud et al., 2005). Even though the infection biology and epidemiology of *G.*

435 *castaneae*, with a few exceptions (Lione et al., 2015; Lione and Gonthier, 2016), are still

436 mostly unknown and, thus, no prior information is available to discriminate which

437 scenario is most likely to occur in nature, the option A seems to fit better to the

438 processes of fungal colonization and oviposition. Moreover, the probability of gathering

439 *in silico* outcomes statistically equivalent to the results gathered from the field trials

440 showed that the hypotheses of equal attractiveness exerted by all the buds towards the

441 fungus/insect are the most likely. These conclusions are supported by the fact that the

442 fungus was isolated from approximately 1/3 of the buds sampled prior to the oviposition

443 period, and also from the buds collected from the site where the oviposition was virtually

444   absent in both samplings. Despite the overall ratio of colonized buds showed a

445   significant increase between the two samplings, the raise was not substantial

446   (approximately +7%) and it was mostly influenced by the data gathered from one out of

447   three sites. Considering that the incidence of *G. castaneae* has been shown to increase

448   with warmer temperatures during the months preceding its assessment (Lione et al.,

449   2015), and provided that in north-western Italy the warmest months of the year are

450   comprised between the two sampling dates (Biancotti et al., 1998), the observed

451   increase could depend on the climate, rather than on the oviposition by *D. kuriphilus*.

452   While the hypothesis of an ecological interaction between *G. castaneae* and *D.*

453   *kuriphilus* during the oviposition stage is not supported, the larger number of adults

454   inhabiting the galls colonized by the fungus suggests the possibility of an interaction

455   occurring subsequently, during the insects development. The fungal mycelium could

456   increase the survival rate of the pests by providing an additional nutritive source for

457   direct consumption (i.e. mycophagy), or by improving the quality of the gall tissues

458   through favorable chemical transformations. The mycelium of *G. castaneae* colonizing

459   the galls might transform plant tissues into a more digestible biomass rich in nutrients.

460   Despite no experimental results can be provided to support these hypotheses, the

461   positive role of fungi on the diet and on the population dynamics of many insects has

462   been largely documented in the literature (Kendrick, 2000; Carlile, 2001). The

463   colonization of galls by *G. castaneae* may also result in a physical alteration of the plant

464   tissues. Several fungi have been shown to induce changes in the firmness of substrates

465   by softening their texture (Kendrick, 2000), which might result in a reduced mechanical

466   resistance leading to an advantage to the insect. However, as noticed by Magro et al.

467   (2010), galls alteration might also be detrimental to *D. kuriphilus*. It is worth noting that

468   since no necrosis or observable physicals alterations were observed on the galls

469   colonized by *G. castaneae* in our study, the role of the fungus as inhibitor of *D.*

470   *kuriphilus* that was suggested by Magro et al. (2010) would deserve further

471   investigations. Moreover, specific studies are needed to clarify whether and how *G.*

472   *castaneae* can modify the galls tissues.

473

474   **5. Conclusion**

475

476   The theoretical approach proposed and used in this study combined the results

477   from different possible ecological interactions between *G. castaneae* and *D. kuriphilus*,

478   while the biological analyses and the validation performed on field data allowed the

479   detection of the most likely hypothesis. All lines of evidence suggest that the ecological

480   interactions between *G. castaneae* and *D. kuriphilus* are asymmetrically favorable to the

481   insect, rather than to the fungus. This is not surprising considering that the two species

482   did not coevolve in their current area of sympatry. It is worth noting that, potentially, the

483   infestations of *D. kuriphilus* could also have increased the spreading ability of the

484   pathogen, since asexual fruiting bodies of *G. castaneae* have been observed on the

485   galls surface (Maresi et al., 2013). However, asexual reproduction has been recently

486   shown to play a minor role compared to sexual reproduction in the spread of the fungal

487   pathogen based on population genetics data (Sillo et al., 2016). Moreover, as

488   documented for other fungi (i.e. latent pathogens), the stress induced on the chestnut

489   by a massive attack of the pest could increase the incidence of the disease (Petrini,

490   1991). Such observations suggest that the level of complexity in the ecological

491   interaction between *G.castaneae* and *D. kuriphilus* might be influenced by other co-

492   occurring factors. However, no studies on these topics are available yet and, to date,

493   our results suggest that the diffusion of *G. castaneae* and the consequent outbreak of

494   the nut rot of chestnut could have boosted the spread of the exotic pest in the newfound

495   area of invasion in Italy.

496

502

503   **References**

504

505   Agresti, A., 2001. Exact inference for categorical data: recent advances and continuing

506   controversies. Stat. Med. 20, 2709–2722.

507   Akaike, H., 1973. Information theory and an extension of the maximum likelihood

508   principle, in: Petrov, B. N., Csaki, F. (Eds.), 2nd International Symposium on Information

509   Theory, Akadémiai Kiadó, Budapest, pp. 267–281.

510   Alma, A., Ferracini, C., Saror, C., Ferrari, E., Botta, R., 2014. Il cinipide orientale del

511   castagno: lotta biologica e sensibilità varietale. Italus Hortus 21, 15–29.

512 Biancotti, A., Bellardone, G., Bovo, S., Cagnazzi, B., Giacomelli, L., Marchisio, C., 1998.

513 Distribuzione Regionale di Piogge e Temperature, CIMA ICAM, Torino.

514 Blaker, H., 2000. Confidence curves and improved exact confidence intervals for

515 discrete distributions. The Can. J. Stat. 28, 793–798.

516 Brussino, G., Bosio, G., Baudino, M., Giordano, R., Ramello, F., Melika, G., 2002.

517 Pericoloso insetto esotico per il castagno europeo. L'Informatore Agrario 37, 59–61.

518 Buckland, S.T., 1983. Monte Carlo methods for confidence interval estimation using the

519 bootstrap technique. J. Appl. Stat. 10, 194–212.

520 Carlile, M.J., Watkinson, S.C., Gooday, G.W., 2001. The Fungi, second ed. Academic

521 Press, London.

522 Carsey, T.M., Harden, J.H., 2014. Monte Carlo Simulation and Resampling Methods for

523 Social Science, SAGE, London.

524 Crawley, M.J., 2013. The R Book, second ed. John Wiley and Sons, Chichester.

525 Danti, R., Della Rocca, G., Panconesi, A., 2013. Cypress canker, in: Gonthier, P.,

526 Nicolotti, G. (Eds.), Infectious Forest Diseases. CAB International, Wallingford, pp. 359–

527 375.

528 Dennert, F.G., Broggini, G.A., Gessler, C., Storari, M., 2015. *Gnomoniopsis castanea* is

529 the main agent of chestnut nut rot in Switzerland. Phytopathol. Mediterr. 54, 199–211.

530 Eckhardt, L.J., 2013. Blackstain root disease and other *Leptographium* diseases, in:

531 Gonthier, P., Nicolotti, G. (Eds.), Infectious Forest Diseases. CAB International,

532 Wallingford, pp. 283–296.

533   Edwards, A.M., 2008. Using likelihood to test for Lévy flight search patterns and for

534   general power-law distributions in nature. J. Anim. Ecol. 77, 1212–1222.

535   EFSA Panel on Plant Health (PLH), 2010. Risk assessment of the oriental chestnut gall

536   wasp, *Dryocosmus kuriphilus* for the EU territory on request from the European

537   commission. EFSA J. 8, 1619.

538   EPPO, 2005. Data sheets on quarantine pests – *Dryocosmus kuriphilus*. EPPO Bull. 35,

539   422–424.

540   Ferracini, C., Gonella, E., Ferrari, E., Saladini, M.A., Picciau, L., Tota, F., Pontini, M.,

541   Alma, A., 2015. Novel insight in the life cycle of *Torymus sinensis*, biocontrol agent of

542   the chestnut gall wasp. BioControl 60, 169–177.

543   Gardes, M., White, T.J., Fortin, A., Bruns, T.D., Taylor, J.W., 1991. Identification of

544   indigenous and introduced symbiotic fungi in ectomycorrhizae by amplification of

545   nuclear and mithocondrial ribosomal DNA. Can. J. Bot. 69, 180–190.

546   Gerber, H.U., Leung, B.P.K., Shiu, E.S.W., 2003. Indicator function and Hattendorff

547   theorem. N.A.A.J. 7, 38–47.

548   Giordano, L., Garbelotto, M., Nicolotti, G., Gonthier, P., 2013. Characterization of fungal

549   communities associated with the bark beetle *Ips typographus* varies depending on

550   detection method, location, and beetle population levels. Myc. Prog. 12, 127–140.

551   Gonthier, P., Lione, G., Giordano, L., Garbelotto, M., 2012. The American forest

552   pathogen *Heterobasidion irregulare* colonizes unexpected habitats after its introduction

553   in Italy. Ecol. Appl. 22, 2135–2143.

554 Griffiths, H.M., 2013. Forest diseases caused by prokaryotes: phytoplasmal and

555 bacterial diseases, in: Gonthier, P., Nicolotti, G. (Eds.), Infectious Forest Diseases. CAB

556 International, Wallingford, pp. 76–96.

557 Happ, G.M., Happ, C.M., Barras, S.J., 1971. Fine structure of the prothoracic

558 mycangium, a chamber for the culture of symbiotic fungi, in the southern pine beetle,

559 *Dendroctonus frontalis*. Tissue Cell 3, 295–308.

560 Harrington, T.C., 2013. *Ceratocystis* diseases, in: Gonthier, P., Nicolotti, G. (Eds.),

561 Infectious Forest Diseases. CAB International, Wallingford, pp. 230–255.

562 Harrison, M.D., Brewer, J.W., Merrill, L.D.,1980. Insect involvement in the transmission

563 of bacterial pathogens, in: Harris, K.F., Maramorosch, K. (Eds.), Vectors of Plant

564 Pathogens. Academic Press, New York, pp. 201–292.

565 Honkaniemi, J., Ojansuu, R., Piri, T., Kasanen, R., Lehtonen, M., Salminen, H.,

566 Kalliokoski, T., Mäkinen, H., 2014. Hmodel, a *Heterobasidion annosum* model for even-

567 aged Norway spruce stands. Can. J. Forest Res. 44, 796–809.

568 Jarnevich, C.S., Young, N., 2015. Using the MAXENT program for species distribution

569 modelling to assess invasion risk, in: Venette, R.C. (Ed.), Pest Risk Modelling and

570 Mapping for Invasive Alien Species. CAB International, Wallingford, pp. 65–81.

571 Jones, C.J., Lawton, J.H., Shachak, M., 1994. Organisms as ecosystem engineers.

572 Oikos 69, 373–386.

573 Jones, O., Maillardet, R., Robinson, A., 2009. Introduction to Scientific Programming

574 and Simulation Using R, CRC Press, Boca Raton.

575 Kato, K., Hijii, N., 1997. Effects of gall formation by *Dryocosmus kuriphilus* Yasumatsu

576 (Hymenoptera: Cynipidae) on the growth of chestnut trees. J. Appl. Entomol. 121, 9–15.

577 Kendrick, B., 2000. The Fifth Kingdom, third ed. Mycologue Publications, Newburyport.

578 Kéry, M., 2010. Introduction to WinBUGS for Ecologists – A Bayesian Approach to

579 Regression, ANOVA, Mixed Models and Related Analysis, Academic Press, London.

580 Kirisits, T., 2013. Dutch elm disease and other *Ophiostoma* diseases, in: Gonthier, P.,

581 Nicolotti, G. (Eds.), Infectious Forest Diseases. CAB International, Wallingford, pp. 256–

582 281.

583 Lachene, B., 2013. On Pearson families of distributions and its applications. Afr. J.

584 Math. Comput. Sci. Res. 6, 108–117.

585 Lione, G., Gonthier, P., 2016. A permutation-randomization approach to test the spatial

586 distribution of plant diseases. Phytopathology 106, 19–28.

587 Lione, G., Giordano, L., Sillo, F., Gonthier, P., 2015. Testing and modelling the effects

588 of climate on the incidence of the emergent nut rot agent of chestnut G*nomoniopsis*

589 *castanea*. Plant Pathol. 64, 852–863.

590 Magro, P., Speranza, S., Stacchiotti, M., Martignoni, D., Paparatti, B., 2010.

591 *Gnomoniopsis* associated with necrosis of leaves and chestnut galls induced by

592 *Dryocosmus kuriphilus.* New Dis. Rep. 21, 15.

593 Maresi, G., Oliveira Longa, C.M., Turchetti, T., 2013. Brown rot on nuts of *Castanea*

594 *sativa* Mill: an emerging disease and its causal agent. *i*Forest 6, 294–301.

595 Mitchell, A., 1999. The ESRI Guide to GIS Analysis – Volume 1: Geographic Patterns &

596 Relationships, ESRI Press, Redlands.

597 Mitchell, A., 2005. The ESRI Guide to GIS Analysis – Volume 2: Spatial Measurements

598 and Statistics, ESRI Press, Redlands.

599 Ôtake, A., 1980. Chestnut gall wasp, *Dryocosmus kuriphilus* Yasumatsu (Hymenoptera:

600 Cynipidae): a preliminary study on trend of adult emergence and some other ecological

601 aspects related to the final stage of its life cycle. Appl. Entomol. Zool. 15, 96-105.

602 Paine, T.D., Raffa, K.F., Harrington, T.C., 1997. Interactions among scolytid bark

603 beetles, their associated fungi, and live host conifers. Annu. Rev. Entomol. 42, 179–

604 206.

605 Pearson, K., 1895. Contributions to the mathematical theory of evolution, II: skew

606 variation in homogeneous material. Philos. Trans. Royal Soc. London 186, 343–414.

607 Petrini, O., 1991. Fungal endophytes of tree leaves, in: Andrews, J.H., Hirano, S.S.

608 (Eds.), Microbial Ecology of Leaves. Springer–Verlag, New York, pp. 179–197.

609 Quacchia, A., Moriya, S., Bosio, G., Scapin, I., Alma, A., 2008. Rearing, release and

610 settlement prospect in Italy of *Torymus sinensis*, the biological control agent of the

611 chestnut gall wasp *Dryocosmus kuriphilus*. BioControl 53, 829–839.

612 Redak, R.A., Purcell, A.H., Lopes, J.R.S., Blua, M.J., Mizell, R.F. III, Andersen, P.C.,

613 2004. The biology of xylem fluid-feeding insect vectors of *Xylella fastidiosa* and their

614 relation to disease epidemiology. Annu. Rev. Entomol. 49, 243–270.

615 Reynolds, A.M., Frye, M.A., 2007. Free-flight odor tracking in *Drosophila* is consistent

616 with an optimal intermittent scale-free search. PLoSONE 2, e354.

617 Sartor, C., Dini, F., Torello-Marinoni, D., Mellano, M.G., Beccaro, G.L., Alma, A.,

618 Quacchia, A., Botta, R., 2015. Impact of the Asian wasp *Dryocosmus kuriphilus*

619 (Yasumatsu) on cultivated chestnut: Yield loss and cultivar susceptibility. Sci. Hortic.

620 197, 454–460.

621 Sieber, T.C., Hugentobler, C., 1987. Endophytische Pilze in Blättern und Ästen

622 gesunder und geschädigter Buchen (*Fagus sylvatica* L.). Eur. J. For. Path. 6, 203–210.

623 Sillo, F., Giordano, L., Zampieri, E., Lione, G., De Cesare, S., Gonthier, P., 2016. HRM

624 analysis provides insights on the reproduction mode and the population structure of

625 *Gnomoniopsis castaneae* in Europe. Plant Pathol. DOI: 10.1111/ppa.12571

626 Somers, R.H., 1962. A new asymmetric measure of association for ordinal variables.

627 Am. Sociol. Rev. 27, 799–811.

628 Spence, N.J., 2001. Virus-vector interactions in plant virus disease transmission and

629 epidemiology, in: Jeger, M.J., Spence, N.J. (Eds.), Biotic Interactions in Plant-Pathogen

630 Associations. CABI Publishing, Wallingford, pp. 15–26.

631 Thébaud, G., Peyrard, N., Dallot, S., Calonnec, A., Labonne, G., 2005. Investigating

632 disease spread between two assessment dates with permutation tests on a lattice.

633 Phytopathology 95, 1453–1461.

634 Tamietti, G., 2016. On the fungal species *Gnomoniopsis castaneae* ("*castanea*") and its

635 synomym *G. smithogilvyi*. J. Plant Pathol. 98, 189–190.

636   Tilman, D., 1999. The ecological consequences of changes in biodiversity: a search for

637   general principles. Ecology 80, 1455–1474.

638   Venables, W.N., Ripley, B.D., 2002. Modern Applied Statistics with S, fourth ed.

639   Springer, New York.

640   Visentin, I., Gentile, S., Valentino, D., Gonthier, P., Tamietti, G., Cardinale, F., 2012.

641   *Gnomoniopsis castanea* sp. nov. (Gnomoniaceae, Diaporthales) as the causal agent of

642   nut rot in sweet chestnut. J. Plant Pathol. 94, 411–419.

643   Webber, J.F., 2004. Experimental studies on factors influencing the transmission of

644   Dutch elm disease. Investigación Agraria: Sistemas y Recursos Forestales 13, 197–

645   205.

646   White, T.J., Bruns, T., Lee, S.J.W.T., Taylor, J.W., 1990. Amplification and direct

647   sequencing of fungal ribosomal RNA genes for phylogenetics, in: Innis, M.A., Gelfand,

648   D.H., Sninsky, J.J., White, T.J. (Eds.), PCR Protocols: a Guide to Methods and

649   Applications. Academic Press, London, pp. 315–322.

650

Figure captions

652   Figure 1. Percentage of buds colonized by *Gnomoniopsis castaneae* (g_o) in the two

653   samplings. The values of g_o observed in sampling 1 (white bars) and sampling 2 (gray

654   bars) are reported separately for each site as well as conjointly for all the sites (i.e.

655   Overall). Different letters on the top of the bars indicate a significant difference (P<0.05)

656   between the g_o values of the two samplings according to the Fisher's exact test. Error

657   bars refer to the 95% confidence interval of g_o.
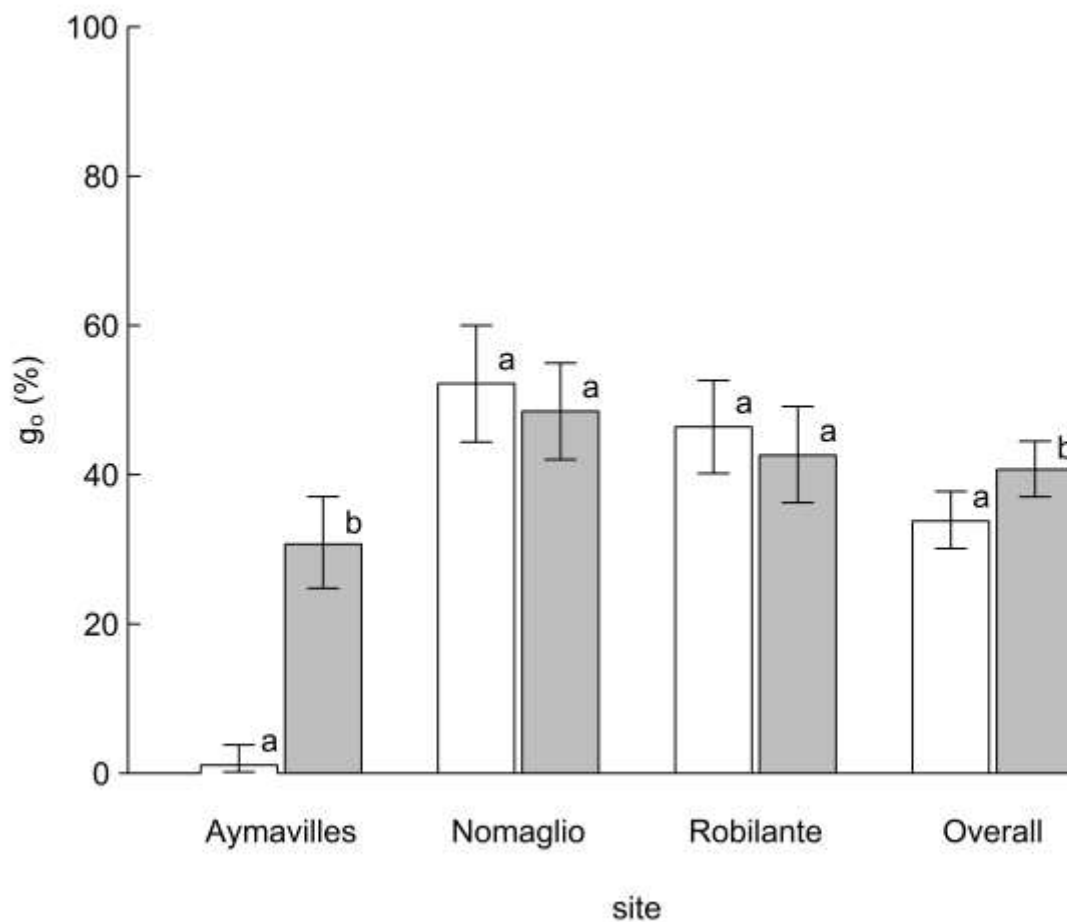
658

659 Table 1. Main characteristics of the sampling sites for the collection of buds and galls of *Dryocosmus kuriphilus* from the

660 European chestnuts.

site	coordinates (UTM WGS84 zone 32N)	elevation (m a.s.l)	aspect	No. of galls sampled	No. of buds sampled (20/06/2013)	No. of buds sampled (25/09/2013)
Aymavilles	361954, 5060322	980	W	175	186	225
Nomaglio	410670, 5043485	580	WSW	124	161	233
Robilante	381836, 4906525	730	WNW	24	250	230

661

662

663 Table 2. Negative binomial generalized linear regression models (nbGLM) comparing the average number of *Dryocosmus*

664 *kuriphilus* adults emerged from galls colonized (GC$^+$) and not colonized (GC$^-$) by *Gnomoniopsis castaneae*. The intercept,

665 the β coefficient and its related P-value are reported for each site and conjointly for all the sites (i.e. Overall). The β

666 coefficients showing a significant difference (P<0.05) between the averages are marked with the symbol *.

667

site	No. of *D. kuriphilus* adults emerged from GC$^+$ (average)	No. of *D. kuriphilus* adults emerged from GC$^-$ (average)	intercept	β	P-value
Aymavilles	3.64	2.89	1.06	0.23*	$3.61 \cdot 10^{-2}$
Nomaglio	3.90	2.00	0.69	0.67*	$4.17 \cdot 10^{-7}$
Robilante	2.62	0.62	-0.47	1.43*	$1.88 \cdot 10^{-4}$
Overall	3.76	2.54	0.93	0.39*	$5.88 \cdot 10^{-9}$

668

669

670 Table 3. Blocks of Monte Carlo simulations defined by the combination of *Gnomoniopsis castaneae* colonization (g) and

671 *Dryocosmus kuriphilus* oviposition (d). The average of the odds ratios $\bar{\theta}$, along with its 95% CI lower and upper bounds

672 ($\bar{\theta}_l$, $\bar{\theta}_u$), are reported for each g-d combination and hypothesis within scenario as measures of association between

673 fungal colonization and oviposition.

674

block		scenario A		scenario B	
g	d	hypothesis A_1	hypothesis A_2	hypothesis B_1	hypothesis B_2
20	20	1.14 (0.17, 3.00)	15.65 (3.70, 50.00)	1.13 (0.18, 2.95)	6.00 (1.68, 15.96)
20	40	0.97 (0.00, 2.60)	20.55 (5.45, 60.57)	1.13 (0.30, 2.90)	5.74 (1.79, 15.44)
20	60	1.14 (0.35, 2.64)	32.05 (7.50, 100.00)	1.13 (0.34, 2.76)	6.00 (1.68, 17.83)
20	80	0.25 (0.00, 1.82)	35.47 (8.00, 85.00)	1.16 (0.38, 2.91)	6.25 (1.60, 22.97)
40	20	1.14 (0.34, 2.75)	15.70 (3.80, 42.16)	1.13 (0.32, 2.68)	9.78 (2.64, 41.17)
40	40	0.93 (0.00, 2.20)	18.35 (5.21, 57.79)	1.08 (0.41, 2.29)	7.18 (2.66, 16.57)
40	60	1.08 (0.44, 2.20)	21.61 (6.91, 56.36)	1.07 (0.44, 2.21)	6.61 (2.54, 15.44)
40	80	0.16 (0.00, 1.48)	26.22 (8.50, 70.30)	1.10 (0.45, 2.25)	6.41 (2.39, 15.28)
50	60	0.15 (0.00, 1.54)	22.61 (6.67, 69.21)	1.08 (0.46, 2.21)	7.81 (3.05, 17.90)

60	20	1.20 (0.36, 2.97)	10.75 (3.23, 17.70)	1.16 (0.37, 2.88)	12.57 (3.38, 21.53)
60	40	0.96 (0.00, 2.28)	17.48 (4.73, 41.13)	1.11 (0.46, 2.34)	13.83 (3.74, 52.04)
60	60	1.10 (0.46, 2.25)	22.61 (5.86, 71.30)	1.09 (0.46, 2.20)	10.75 (3.64, 29.06)
60	80	0.16 (0.00, 1.47)	26.17 (6.91, 102.50)	1.07 (0.46, 2.14)	8.75 (3.32, 19.78)
80	20	1.39 (0.30, 5.45)	4.78 (2.24, 6.25)	1.35 (0.34, 5.68)	6.58 (3.08, 7.90)
80	40	1.22 (0.37, 3.33)	9.80 (3.51, 14.29)	1.20 (0.40, 2.96)	14.49 (4.83, 20.24)
80	60	0.13 (0.00, 1.48)	9.52 (3.30, 14.05)	1.14 (0.40, 2.57)	20.83 (5.44, 38.84)
80	80	0.15 (0.00, 1.54)	19.37 (5.47, 40.00)	1.13 (0.39, 2.51)	21.86 (5.25, 60.80)

675

676

677